THERMAL ENTROPY PRODUCTION AS A KEY TO UNDERSTANDING UNCERTAINTIES IN GEOTHERMAL SYSTEMS

J. Florian Wellmann[1] and Klaus Regenauer-Lieb[1,2]

[1]CSIRO Earth Science and Resource Engineering, 26 Dick Perry Ave., Kensington WA 6151, Australia

[2]School of Earth and Environment, The University of Western Australia, 35 Stirling Hwy, Crawley, WA 6009, Australia

florian.wellmann@csiro.au

Keywords: *Uncertainty, Geothermal Systems, Thermal Entropy Production*

ABSTRACT

Simulations of subsurface temperature usually contain uncertainties and an important question is then: exactly how uncertain are they, or how well are we able to predict them? We propose here that the uncertainty is depending on the main heat transport mechanisms: if heat transported by conduction only, then the temperatures are relatively simple to predict and the uncertainty is low. However, if advective heat transport is present, then the additional transport of heat in the fluid phase can significantly change the temperature field, making it more difficult to predict.

We suggest here a method that enables us to evaluate the dominating heat transport mechanisms with a method based on the thermodynamic concept of entropy production.

Simple examples show that the internal thermal entropy production is zero if a system is in a conductive steady state. If convection is present in the system, entropy production is greater than zero, with higher values for more vigorous convection. In fact, for a simple layer system, it can be shown that the entropy production is directly related to the efficiency of heat transport, measured with the Nusselt number.

We conclude from these examples that thermal entropy production can be applied to estimate how well we will be able to predict temperatures in a specific geothermal resource area.

1. INTRODUCTION

Uncertainties in simulations of subsurface processes are commonly evaluated with stochastic simulations (e.g. Doherty, 1994; Subbey et al., 2004; Riva et al., 2010; Vogt et al., 2010a). Instead of one specific result, a variety of probable realisations are generated, within the range of input data or parameter uncertainty. As a large quantity of simulation results are generated with these methods, effective measures are required to identify and classify the results. The aim of the work presented here is to evaluate whether a thermodynamic measure can be applied to classify simulated flow fields in coupled hydrothermal systems.

A variety of methods has already been developed to evaluate results of stochastic simulations. The main scope of such analyses is to evaluate how accurately the simulation can predict a set of observables, for example temperatures at observation points (e.g. Vogt et al., 2010b), or the production history in an oil reservoir (Suzuki et al., 2008). Even, though, these methods are well suited for typical problems of calibration and production forecast, they do not provide a measure of the state of the whole system.

In the work presented here, it will be evaluated if a thermodynamic measure, specific thermal entropy production, can be applied to characterize the system state. In the classical sense, thermodynamic measures can be applied to predict the response of a system with macroscopic measures, without having to know all the detailed processes within the system. A simple and typical example is the "Ideal Gas Law", describing the relationship between pressure P, temperature T and volume V in an ideal gas:

$$PV = Nk_BT \quad ,$$

where N is the number of molecules in the gas and the proportionality factor k_B the Bolzmann's constant. Based on the kinetic theory of gases, this formula can be used to evaluate how, for example, a volume change affects temperature – without having to know the kinetic energy of every single molecule in the gas. On the appropriate scale and for a specific question, thermodynamic measures are useful to describe systems without having to know exactly the details inside the system itself.

Based on these considerations, it will here be evaluated if thermal entropy production is useful as a measure of the thermodynamic state of a hydrothermal flow system.

2. THERMAL ENTROPY PRODUCTION IN A THERMO-HYDRAULIC SYSTEM

Entropy production is related to dissipative heat processes within a system. The entropy of a diabatic system changes if heat is supplied or removed from the system. The change of entropy, the entropy production, is defined as the ratio between the change in heat Q and the temperature T (e.g. Callen, 1985):

$$\dot{S} \equiv \frac{\delta Q}{T}$$

The second law of thermodynamics states in the traditional (non-statistical) form that entropy in a closed system is either constant or increases and therefore:

$$\dot{S} \geq 0 \quad .$$

Entropy is produced due to reversible and irreversible processes (see Regenauer-Lieb et al., 2010, and references therein). Here, only the entropy production for slow fluid flow in a permeable matrix is considered, using an approach initially developed for climate systems. For a thermo-hydraulic system that exchanges heat with its surroundings, the entropy production $\dot{S}$ for the system and its surroundings can be described as:

$$\dot{S} = \int_V \frac{1}{T}\left[\frac{\partial(\rho c_P T)}{\partial t} + \nabla\cdot(\rho c_P T \vec{v}_f) + p\nabla\cdot\vec{v}\right]dV + \oint_A \frac{1}{T}\vec{q}_h\cdot\vec{n}dA$$

The volume integral on the right side describes entropy production within the system due to viscous dissipation, considering fluid density ρ and heat capacity c_P, temperature T and pressure p, and the fluid velocity $\vec{v}$.

The surface integral represents entropy production due to thermal dissipation for a heat flux q_h, perpendicular to a surface A ($\vec{n}$ is the normal vector on the surface).

If we only consider thermal dissipation, and assume that the internal system is in steady state (in a statistical sense), the entropy production is reduced to the heat that is supplied through the boundary by the heat flux q (Ozawa et al., 2003):

$$\dot{S} = \oint_A \frac{1}{T}\vec{q}_h\cdot\vec{n}dA$$

Only the conductive heat transport is considered here as relevant to entropy production. This is following the argument of Ozawa et al. (2003) that advective heat transport is, in principle, a reversible process and does therefore not contribute to viscous dissipation. However, advective heat transport implicitly induces entropy production as it can lead locally to very large temperature gradients, and therefore induces conductive processes.

As the entropy production, defined in the description in the equation above, depends on the size of the subsystem through the integration over the surface, it can be scaled by the mass $V\rho$ of the system to obtain the specific entropy production:

$$\dot{s} = \frac{\dot{S}}{V\rho}$$

As a measure of the whole entropy production in a larger system, the average specific entropy production can be calculated:

$$\langle \dot{s} \rangle = \frac{1}{V}\int_V \dot{s}dV$$

3. APPLICATION OF ENTROPY PRODUCTION TO ANALYSE A TRANSIENT CONDUCTIVE HEAT FLOW FIELD

3.1 Basic considerations for the conductive case

As a first example, the average specific entropy production for a system in a transient conductive state will be evaluated. In the following considerations, conductive heat fluxes are aligned with coordinate axes. The fluxes are per definition oriented towards the system. From these considerations directly follows that the entropy production of a system in conductive steady state is zero as all heat fluxes into and out of the system are completely balanced. For example, considering a simple system with a vertical heat flux only, no heat flux in or out of the cell exists in x-direction and the same applies to the y-direction. The heat flux in z-direction is the same into and out of the cell $q_{z,in} = q_{z,out}$. Therefore, the internal entropy production is zero.

3.2 Entropy production in a transient conductive system

We will now consider a system that initiates from a conductive steady state but then experiences a change in the boundary conditions. The system is a conductive porous medium in a rectangular box with a thickness of 2500 m and a lateral extent of 3000 x 3000 m. Temperature is fixed at the top (10°C) and the system is homogeneous and isotropic, with a thermal conductivity of λ = 2.9 W $K^{-1}m^{-1}$ and a thermal diffusivity of $\kappa = 10^{-6}m^{-2}$. Lateral no flux boundary conditions apply. We perform a numerical experiment to determine the temperature profile within the box using the finite-difference simulation code SHEMAT (Clauser and

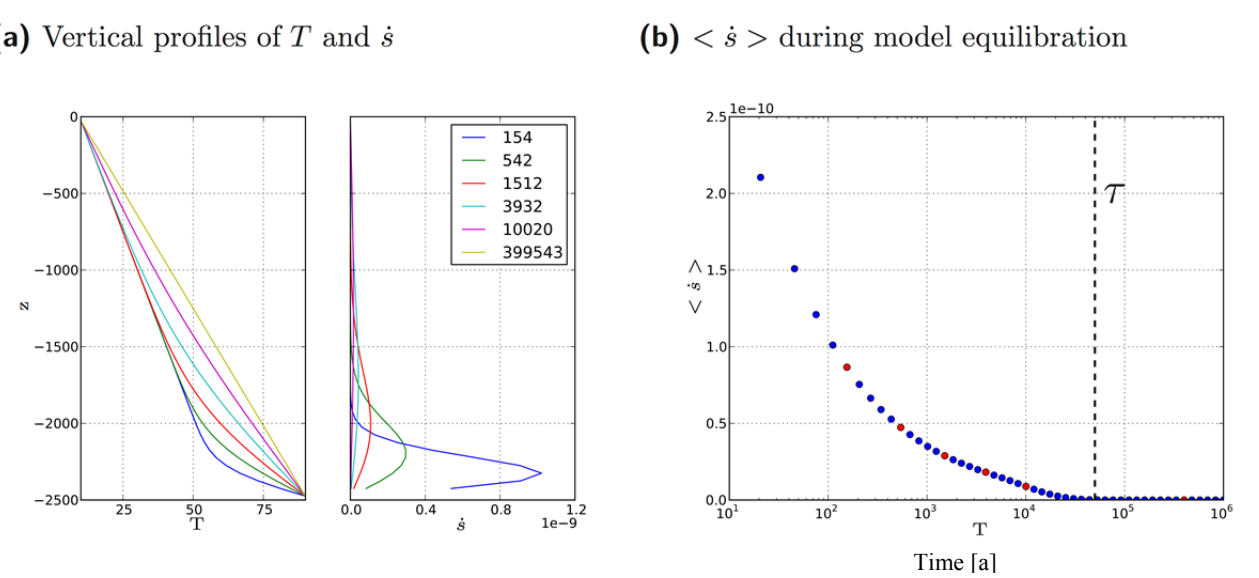

Figure 1: Entropy production during equilibration phase in a conductive system starting from a steady state; (a) Vertical profiles of temperature and entropy production in the simulated box for different times (in years, see legend); (b) average specific entropy production in the entire box, decreasing back to zero during the time of the experiment. The dashed line indicates the theoretical characteristic time scale.

Bartels, 2003). The box is discretised into a regular mesh with cell sizes of 100 m in x- and y-direction, and 50 m in z-direction. The specific entropy production for every cell in the domain is calculated from the heat flux over all cell surfaces, and the average specific entropy production is calculated with the equations given above.

The system is initially in a conductive steady state with a temperature at the base of 60°C. Then, temperature at the base is instantaneously increased to a higher value of 90°C. The high temperature at the base will lead to transient conductive effects in the system until a new steady state is reached. This equilibration time span is simulated here with 50 logarithmically spaced time steps for a total time of 10^6 years. With the parameters of the transport problem considered here, the system equilibration can be evaluated from the characteristic time scale τ of diffusive heat transport (e.g. Turcotte and Schubert, 2002):

$$\tau = \frac{1}{2\kappa} l^2 \approx 50{,}000 \text{ years.}$$

It can therefore be expected that the system reach the steady state in the time scale of the simulation.

In figure 1a, vertical profiles of temperatures and entropy production for different times after the temperature increase are presented. The temperature profiles reflect the sudden temperature increase at the base and the subsequent propagation of the temperature front towards the top of the system. The profile of specific entropy production shows that the entropy production is maximal in the region of the system where the temperature front propagates. The peak itself is decreasing over time as the temperature front becomes broader.

The temporal development of the average specific entropy production over time (fig. 1b) shows that entropy production is initially very high in the system and then subsequently decreases back to zero when the system reaches the new steady state. The high increase at the beginning is due to the high temperature contrast at the base of the system. The new equilibrium state is reached after approximately 10^5 years. This is in the order of the characteristic time scale τ of the system, indicated with the vertical dotted line in figure 1b.

This simple example showed that the average entropy production could be applied to evaluate the internal thermodynamic state of a conductive system during the equilibration phase. The time scale for equilibration and the decrease of the value to zero are in accordance to theoretical considerations. In the next step, the application of the measure to visualize and analyze more complex systems is evaluated.

4. ANALYSIS OF ENTROPY PRODUCTION IN A CONVECTIVE SYSTEM

4.1 Relationship between thermal entropy production and advective heat transport

As a second example, we examine how entropy production within the system is affected by advective heat transport with a simple convective system heated from below (fig. 2). Heat is transported with the fluid in the upwelling and downwelling parts of the convection cell, leading to the typical temperature profile of a convection system (background picture in fig. 2).

We consider now the processes in a small sub-part of the system where colder fluid is transported downwards. The advecting fluid disturbs the temperature field and leads to a temperature gradient between adjacent sub-volumes in the system. This temperature gradient causes a conductive heat flow q_x between from the hotter to the colder volume, with temperatures T_H and T_C. This heat flow leads to an entropy change in both systems:

$$\dot{S}_H = \frac{-q_x}{T_H} < 0 \quad \text{and} \quad \dot{S}_C = \frac{q_x}{T_C} > 0$$

It is interesting to note that the entropy is decreased in the hotter sub-volume but increased in the colder system. However, this is not a violation of the second law of thermodynamics because each sub-volume is not a closed system. Also, considering the two subvolumes, the average entropy of this small subsystem is increased:

$$\left\langle \dot{S}_{HC} \right\rangle = \dot{S}_H + \dot{S}_C > 0$$

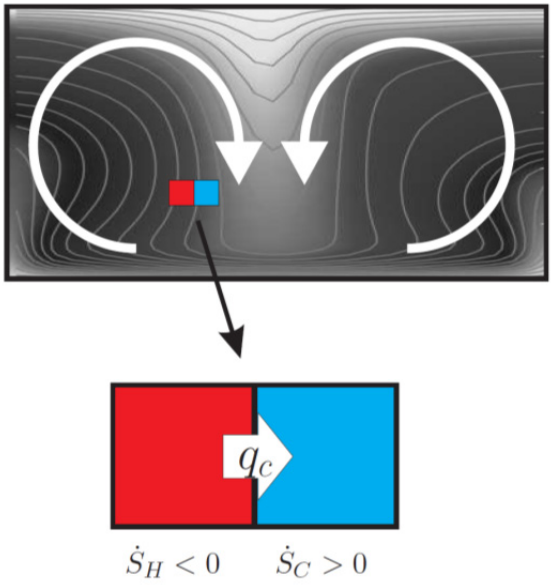

Figure 2: Thermal entropy production in a convective system: if a cool fluid parcel is transported downwards in a convection cell, it is getting in contact with a warmer parcel, invoking a heat flux and increasing the entropy production

This simple consideration indicates that entropy production is non-zero in a convective system because temperature disturbance due to advective heat transport leads to an increase in entropy. Furthermore, it can be expected that entropy production increase with more vigorous convection. A measure commonly applied to determine the heat transport through a system is the non-dimensional Nusselt number, the ratio between the total heat flow to conductive heat flow:

$$Nu = \frac{q_T}{q_c}$$

For the case of pure conduction, $q_T = q_c$ and the Nusselt number is 1. In a convective system, the Nusselt number is greater than 1 and increases with more vigorous convection (Nield and Bejan, 2006). Regenauer-Lieb et al. (2010) showed that the Nusselt number can be related to the thermal dissipation in a system. Specifically for the case considered here, the Nusselt number can be expected to be proportional to the thermal entropy production in the system

$$Nu \propto \dot{S},$$

suggesting that higher entropy production can be related to a higher heat transfer rate through the system, which, for the case of a convective system, is associated with higher fluid velocities (e.g. Nield and Bejan, 2006).

4.2 Entropy production during the onset of convection

In analogy to the study of the conductive system presented before, we want to evaluate if the average entropy measure can be used to determine the state of the system from conductive to convective equilibrium state. We perform again a numerical experiment with the same specifications as in Sec. 3.2, and additionally consider fluid transport in the box. Similar to before, the average specific entropy production is calculated for every time step. The average specific entropy production curve for the onset of convection in the porous system with a permeability of $5 \cdot 10^{-13}$ m^2 as used in the example above, is presented in figure 3. The system initiates from a conductive steady state with no entropy production. When convection sets in, entropy production reaches a maximum and then decreases and converges to a finite value larger than zero, in accordance to what was expected from the theoretical considerations above.

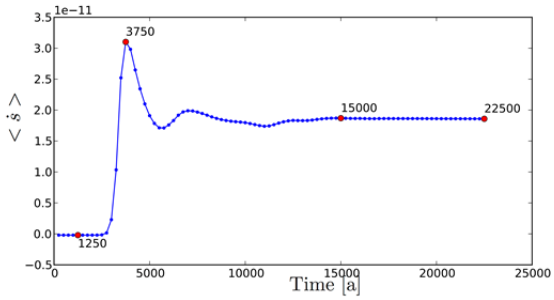

Figure 3: specific thermal entropy production during the onset of convection in a porous medium. After the convective system is developed, the system reaches a convective equilibrium state with non-zero entropy production

This example shows that the average entropy production provides an insight into the global behavior of the system between two equilibrium states. We will now evaluate how the behavior changes with different system properties. As evaluated before, the onset of convection in the system can be expected for permeabilities larger than approximately $1.25 \cdot 10^{-13}$ m^2. In the following experiment, we will evaluate the entropy production in the same system for a range of different permeabilities, from 10^{-13} m^2 to 10^{-11} m2. All other parameters and settings are kept constant.

Graphs for the average specific entropy production during the onset of convection in these models are presented in figure 4. The specific entropy production for a permeability of 10^{-13} m^2 remains zero, indicating that the system stays in a conductive steady state. For higher values, convection sets in and the same pattern is observed as before, with an increase of entropy production during the onset of convection, leveling out to a constant finite value when the system reaches the convective equilibrium state. Due to a higher heat transfer in the system, the onset of convection occurs at earlier times for systems with higher permeabilities. For very high permeabilities, flow velocities become too high for the grid resolution considered here.

4.3 Relationship between Nusselt number and entropy production

In the experiment shown in figure 4, it was observed that the finite values of entropy production in convective systems increase for convection in higher permeable layers (fig. 4). We will now evaluate the relationship between entropy production and Nusselt number in this system.

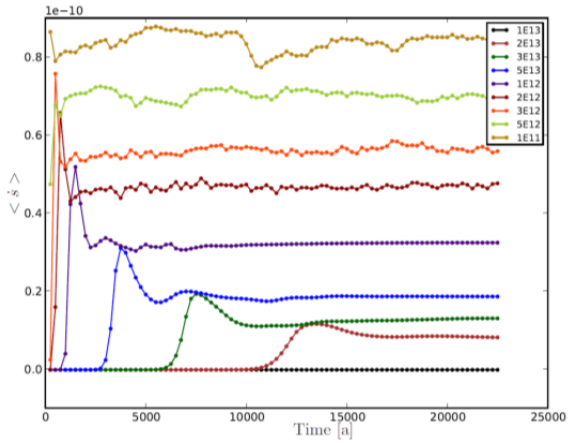

Figure 4: specific entropy production during the onset of convection for multiple scenarios with different premeabilities of the porous layer

The non-dimensional Nusselt number is defined as the ratio of total heat flow (advective and conductive) to conductive heat flow. For a homogeneous system of equal thickness with impermeable boundaries as considered here, the Nusselt number can be estimated from the ratio of the mean temperature gradient over the boundary to the temperature gradient over the whole system (e.g. Holzbecher, 1998):

$$Nu \approx \frac{\frac{1}{L}\int_L \frac{\partial T}{\partial z} dx}{\frac{T_{\max} - T_{\min}}{H}},$$

where T_{max} and T_{min} are fixed temperatures at bottom and top of the system, L the area of the base of the system and H its thickness. Applying this method to the last time step of the convection simulations presented above (fig. 4), we obtain an estimation of Nusselt numbers in the system and can compare these to the average specific entropy production, presented in figure 5.

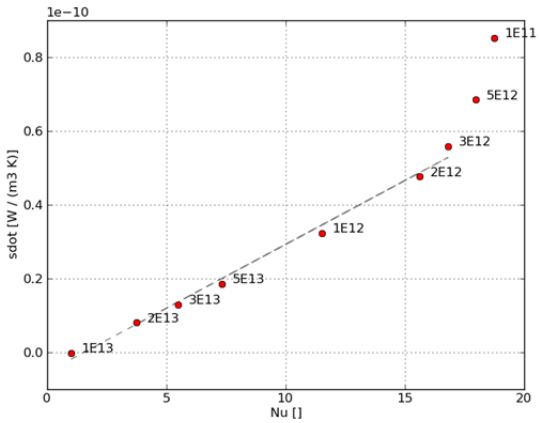

Figure 5: relationship between the experimentally determined equilibrium state of thermal entropy production (sdot) and the Nusselt number (Nu) suggesting a linear relationship

The results show a correlation between Nusselt number and entropy production, with a clear linear relationship for the lower permeability scenarios, up to $k = 2 \cdot 10^{-13}$ m^2. Since inertial terms are neglected in our calculations, we attribute the deviation for higher permeabilities to numerical instabilities. Nevertheless, the proportionality between Nusselt number and entropy production as expected from theory (Regenauer-Lieb et al., 2010) is obtained in the results of the numerical study, providing an indication for the suitability of the measure to classify the thermodynamic state of the system.

5. DISCUSSION

The results show that average thermal entropy production can be applied as a measure to compare the thermodynamic state of a coupled hydrothermal system. Thermal entropy production describes the state of a system with respect to applied boundary conditions, through a comparison of heat transport into and out of the system. If a system is in steady state, entropy production converges to a stable value. Specifically, if a system is in a conductive steady state, then the entropy production is 0. The example simulations show that entropy production increases during the onset of convection, but then decreases again as the system stabilizes and converges to a finite value.

The relationship between thermal entropy production and the hydrothermal state of the system is, in our point of view, an important step towards an analysis of uncertainties in geothermal systems on the scale of the entire system: the higher the thermal entropy production in the system, the more difficult it will generally be to predict its state (e.g. temperatures at each location). A formal evaluation of this relationship is the scope of further research.

REFERENCES

Callen, B. H., 1985. Thermodynamics and an Introduction to Thermostatistics. Vol. 66. Wiley, New York.

Clauser, C., Bartels, J., 2003. Numerical simulation of reactive flow in hot aquifers: SHEMAT and processing SHEMAT. Springer, Berlin..

Doherty, J., 1994. PEST: a unique computer program for model-independent parameter optimisation. Water Down Under 94: Groundwater/Surface Hydrology Common Interest Papers; Preprints of Papers, 551.

Holzbecher, O. E., 1998. Modeling density-driven flow in porous media: principles, numerics, software. Springer, Berlin.

Nield, A. D., Bejan, A., 2006. Convection in porous media. Springer Verlag.

Turcotte, L. D., Schubert, G., 2002. Geodynamics, 2nd Edition. Cambridge University Press, Cambridge.

Ozawa, H., Ohmura, A., Lorenz, D. R., Pujol, T., 2003. The second law of thermodynamics and the global climate system: a review of the maximum entropy production principle. Rev. Geophysics 41 (4), 1018.

Regenauer-Lieb, K., Karrech, A., Chua, T. H., Horowitz, G. F., Yuen, D., 2010. Time- dependent, irreversible entropy production and geodynamics. Philosophical Transactions of the Royal Society A: Mathematical, Physical and Engineering Sciences 368 (1910), 285.

Riva, M., Guadagnini, L., Guadagnini, A., 2010. Effects of uncertainty of lithofacies, conductivity and porosity distributions on stochastic interpretations of a field scale tracer test. Stochastic Environmental Research and Risk Assessment 24 (7), 955–970.

Suzuki, S., Caumon, G., Caers, J., 2008. Dynamic data integration for structural modeling: model screening approach using a distance-based model parameterization. Computational Geosciences 12 (1), 105–119.

Vogt, C., Mottaghy, D., Wolf, A., Rath, V., Pechnig, R., Clauser, C., 2010a. Reducing temperature uncertainties by stochastic geothermal reservoir modelling. Geophysical Journal International 181 (1), 321–333.

Vogt, C., Mottaghy, D., Wolf, A., Rath, V., Pechnig, R., Clauser, C., 2010b. Reducing temperature uncertainties by stochastic geothermal reservoir modelling. Geophysical Journal International 181 (1), 321–333.